

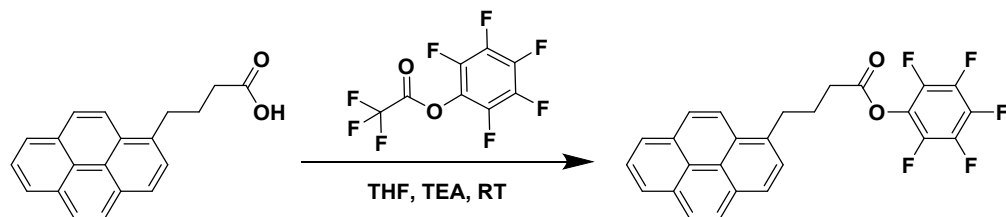
Supporting Information for

Conductive hydrogel composites with autonomous self-healing properties

Xiaohui Li,^{a,b} Xia Huang,^{a,b} Hatice Mutlu,^b Sharali Malik^c and Patrick Theato *^{a,b}

- a. Institute for Chemical Technology and Polymer Chemistry (ITCP), Karlsruhe Institute of Technology (KIT), Engesserstr.18, D-76131 Karlsruhe, Germany
- b. Soft Matter Synthesis Laboratory, Institute for Biological Interfaces III (IBG 3), Karlsruhe Institute of Technology (KIT), Herrmann-von-Helmholtz-Platz 1, D-76344 Eggenstein-Leopoldshafen, Germany
- c. Institute of Quantum Materials and Technology, Karlsruhe Institute of Technology (KIT), Hermann von Helmholtz Platz 1, D-76131 Karlsruhe, Germany

1. Synthesis of perfluorophenyl 4-(pyren-1-yl) butanoate



Scheme S1. The synthesis route of perfluorophenyl 4-(pyren-1-yl) butanoate.

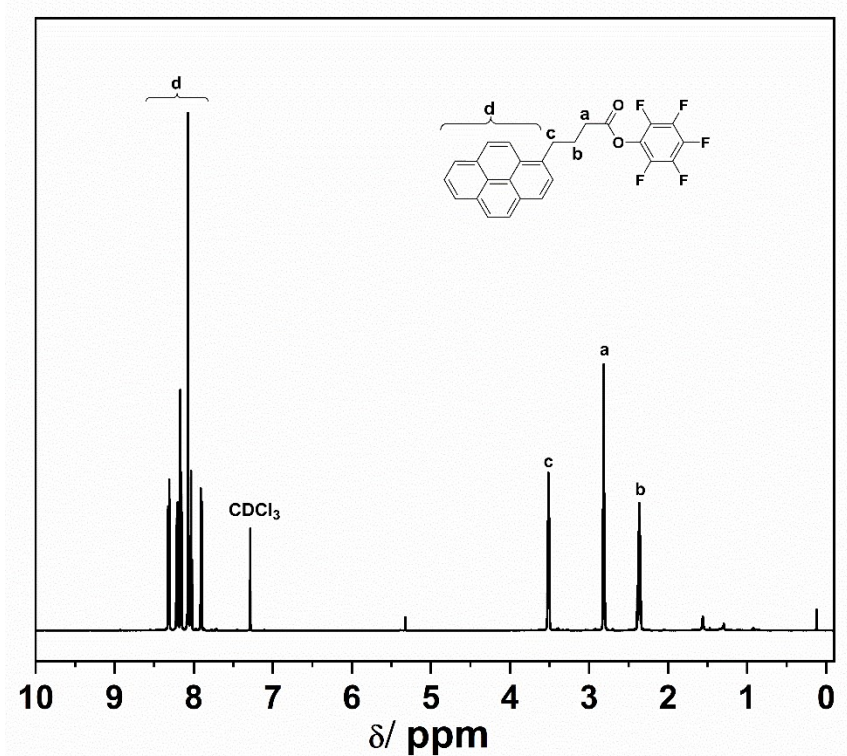


Figure S1. The ^1H -NMR (400 MHz) spectra of perfluorophenyl 4-(pyren-1-yl) butanoate in CDCl_3 .

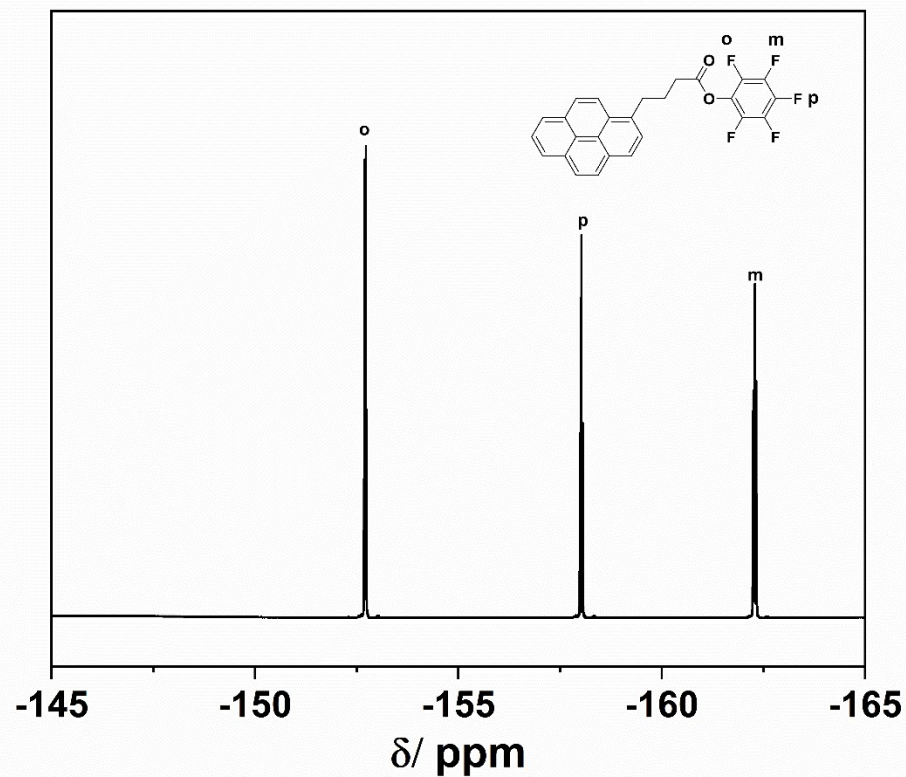
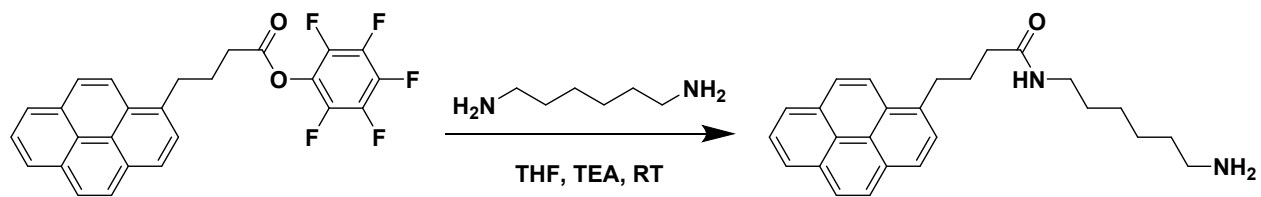


Figure S2. The ^{19}F -NMR (377 MHz) spectra of perfluorophenyl 4-(pyren-1-yl) butanoate in CDCl_3 .

2. Synthesis of N-(6-aminohexyl)-4-(pyren-1-yl) butanamide (APB)



Scheme S2. The synthesis route of *N*-(6-aminohexyl)-4-(pyren-1-yl) butanamide (APB).

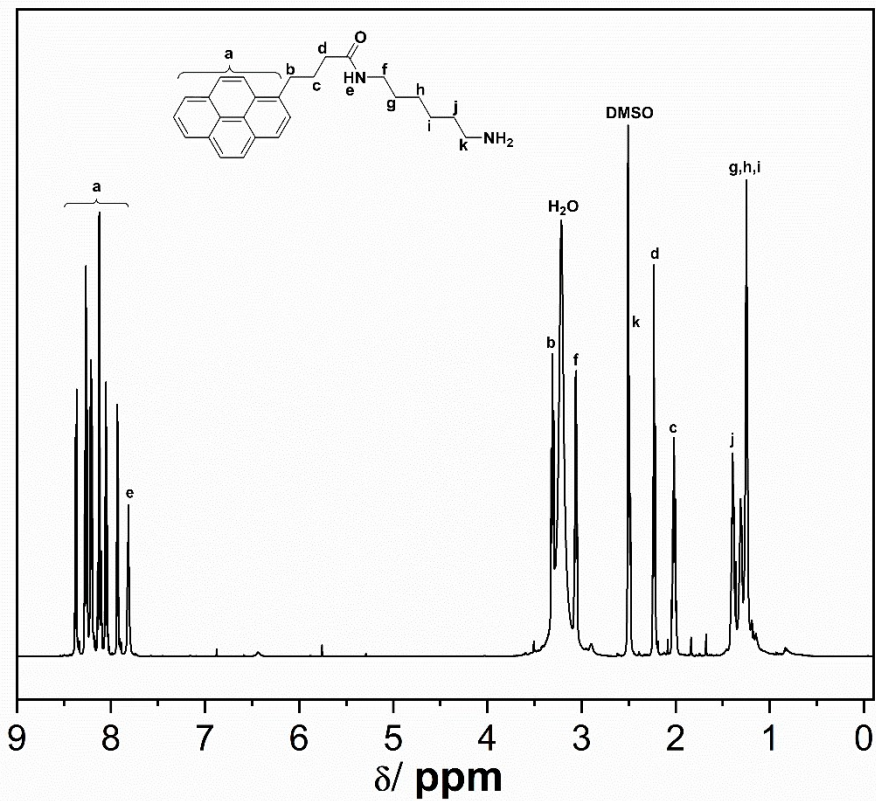


Figure S3. The ^1H -NMR (400 MHz) spectra of *N*-(6-aminohexyl)-4-(pyren-1-yl) butanamide (APB) in $\text{DMSO}-d_6$.

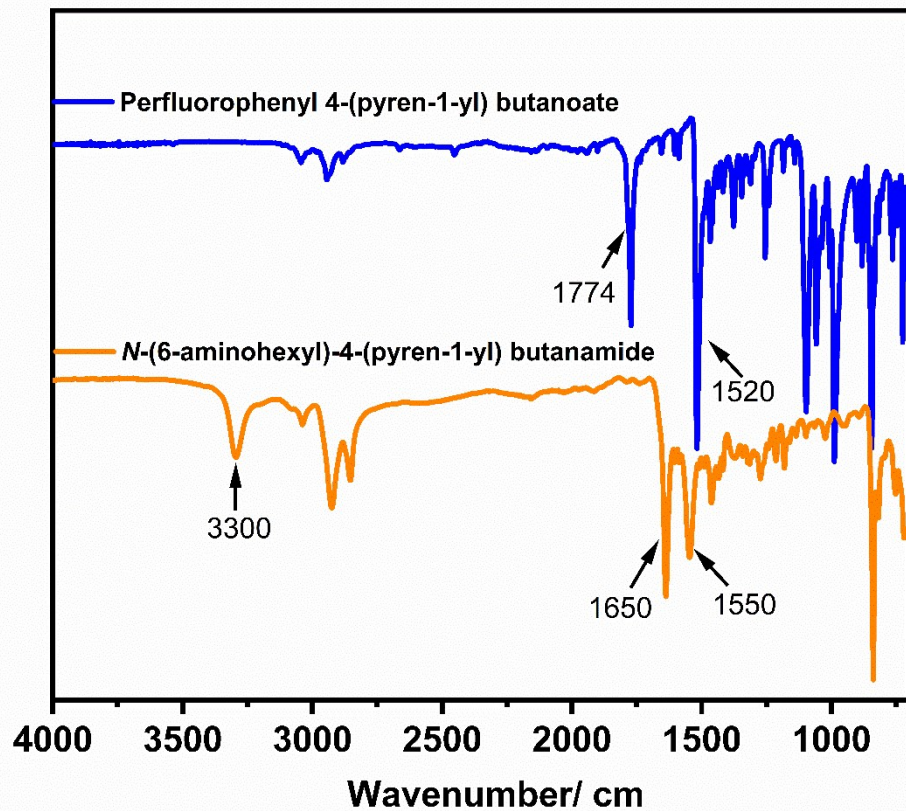


Figure S4. The FT-IR spectra of perfluorophenyl 4-(pyren-1-yl) butanoate and *N*-(6-aminohexyl)-4-(pyren-1-yl) butanamide (APB).

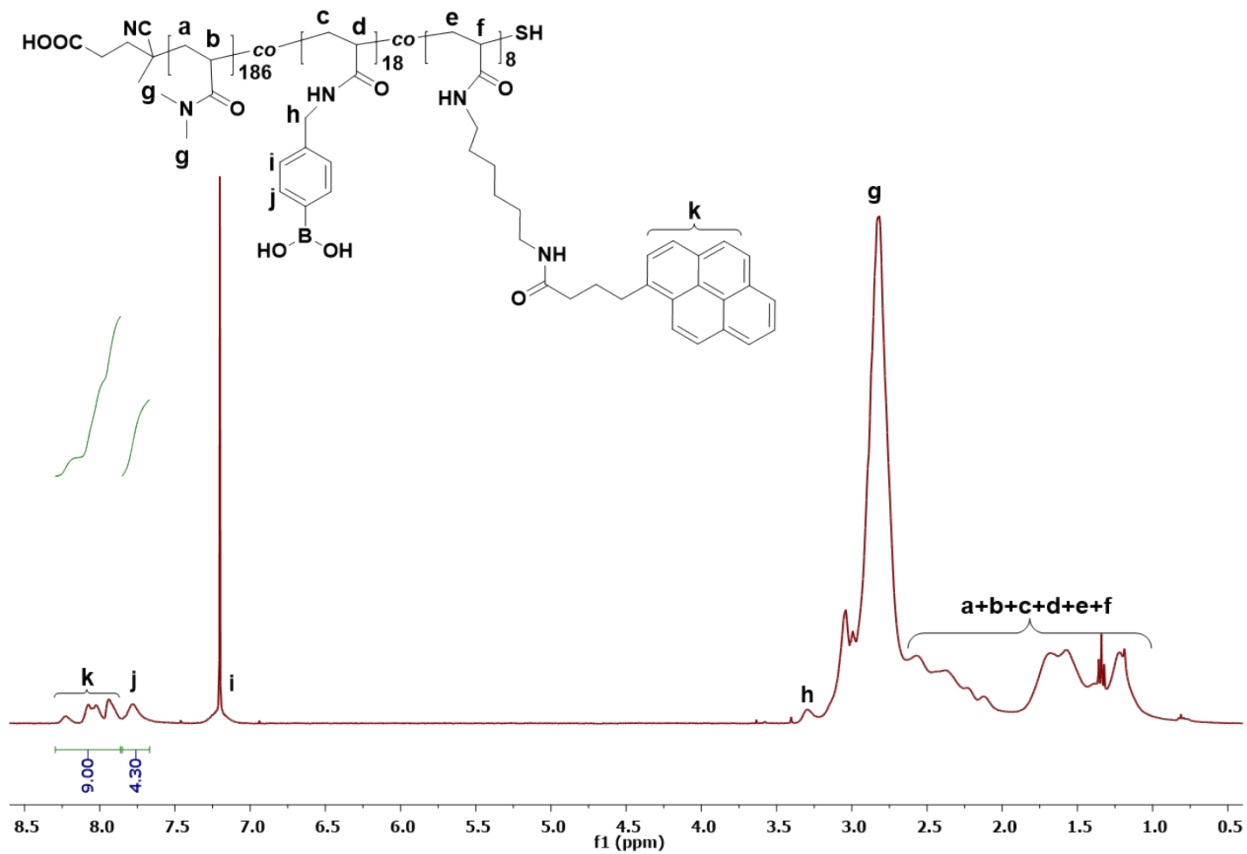


Figure S5. The ^1H -NMR (400 MHz) spectra of P(DMA-co-APB-co-PBA), i.e. P2, with detailed integral information.

Sample	After sonication	1 week	2 weeks	1 month
Sample A				
Sample B				

Figure S6. Photographs of SWCNTs aqueous suspension without and with P2, respectively sample A and B, after sonication 20 min, one week, two weeks and one month.

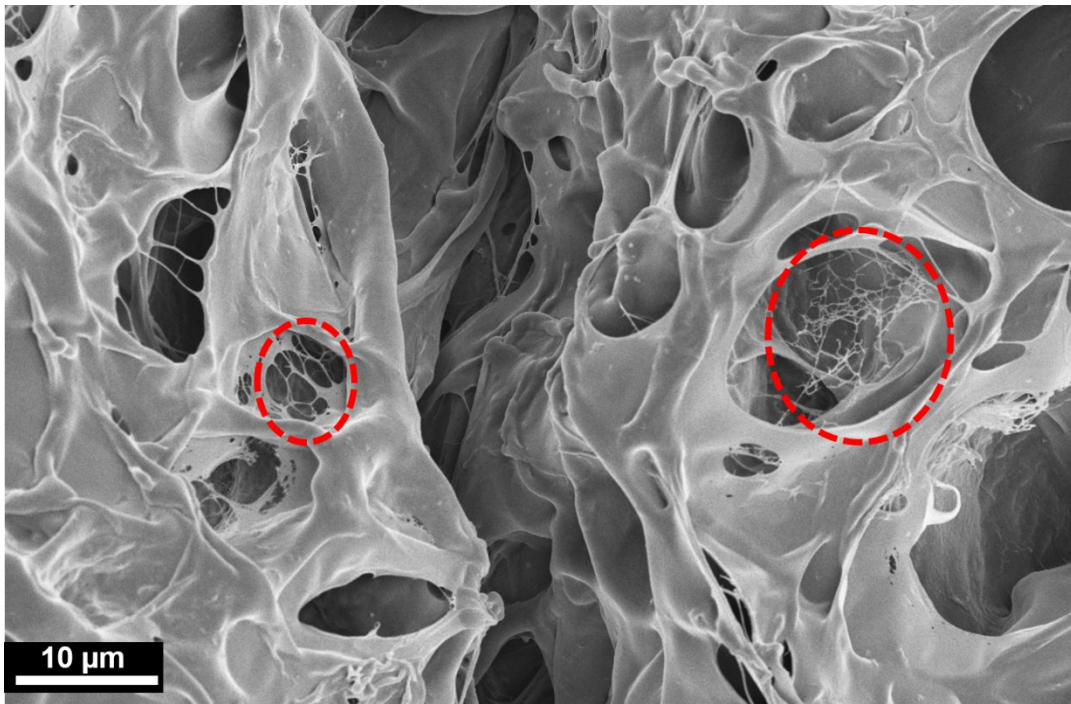


Figure S7. SEM image of the freeze-dried hydrogel formed at neutral pH, and micro-fibrils were highlighted in the red cycles.

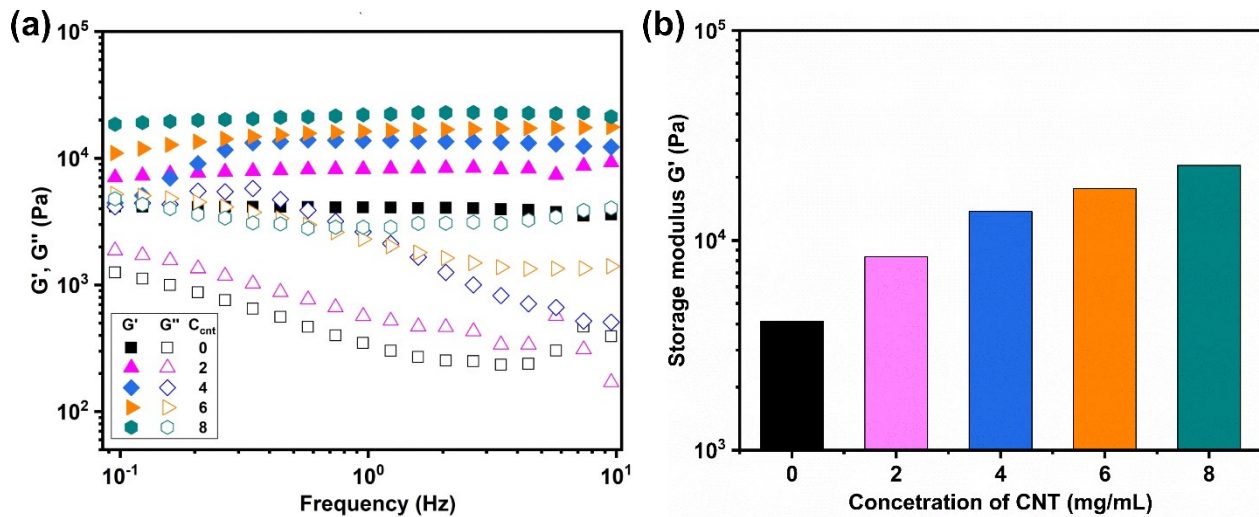


Figure S8. (a) Frequency sweep measurements of hydrogels with different SWCNTs concentration (2, 4, 6, and 8 mg/mL). (b) The plateau of storage modulus G' of the hydrogels with different SWCNT concentration (2, 4, 6, and 8 mg/mL).

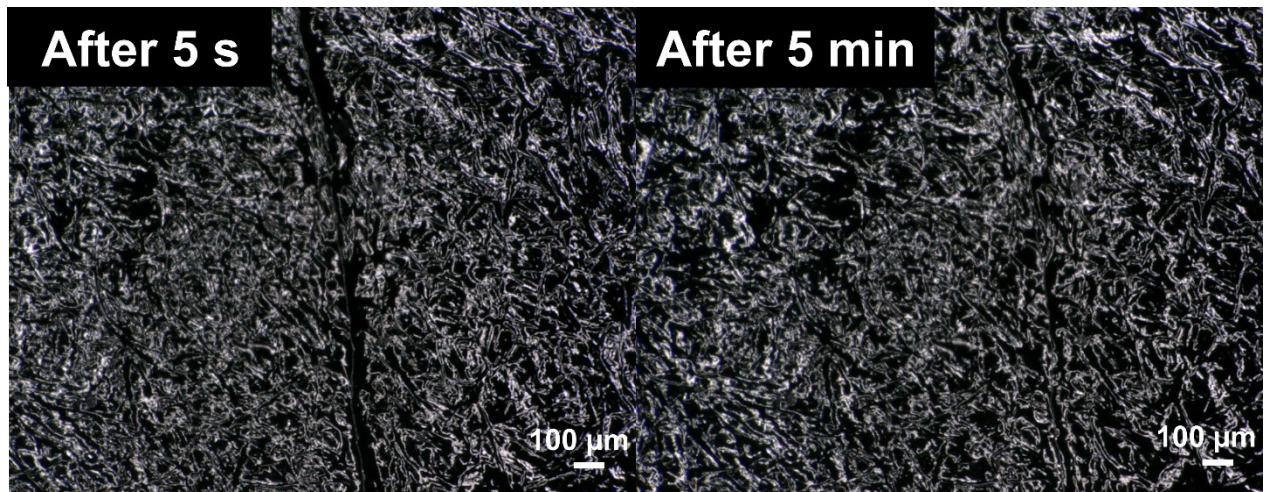


Figure S9. Optical microstructures of the damage site after healing for 5 s and 5 min.

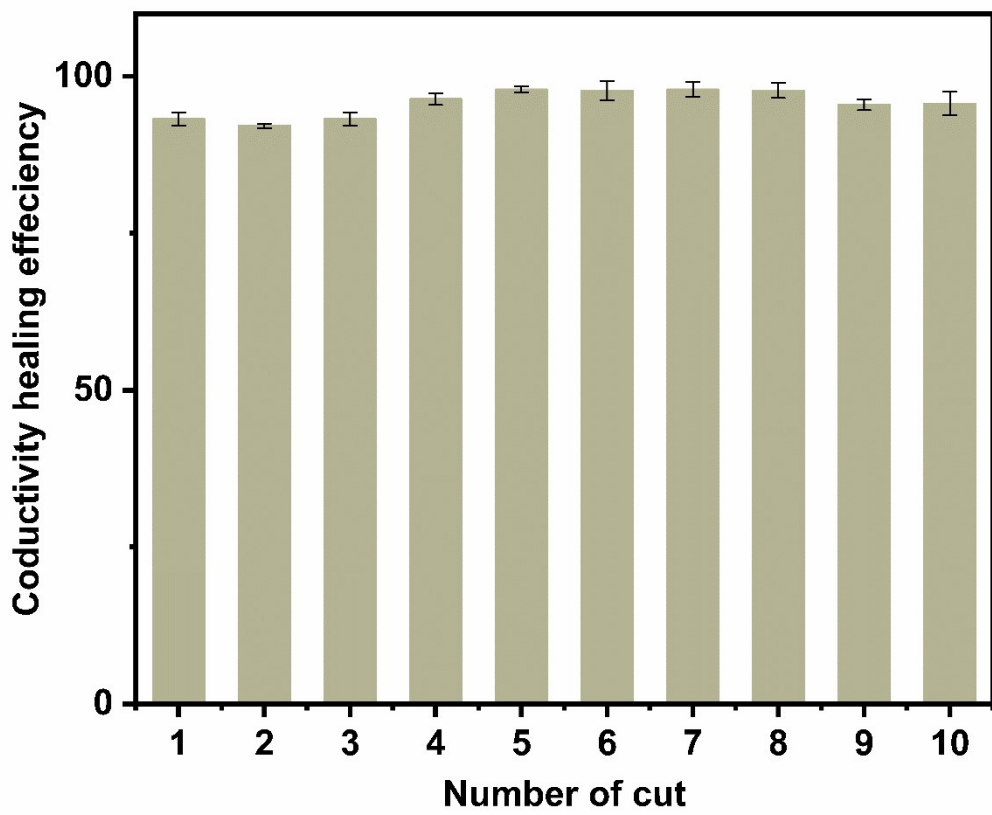


Figure S10. The electrical conductivity healing efficiency within ten cut-and-heal cycles.

Table S1. Typical conductive and self-healable hydrogels and their corresponding conductivities.

Nr.	Hydrogel system ^a	Self-healing mechanism	Conductivity	Ref.
1	PVA/borax/FSWCNTs	Boronate ester bonding	$\sim 1.4\text{--}4.5 \times 10^{-4}$ S/cm	1
2	PVA/CMC-B(OH) ₂	Boronate ester bonding	$\sim 1.5\text{--}3.7 \times 10^{-3}$ S/cm	2
3	PVA/PDMA-B(OH) ₂ /SWCNTs	Boronate ester bonding	$0.3\text{--}1.27 \times 10^{-2}$ S/cm	Present work
4	PEG/PAMAA-Fe ³⁺	Metal ion coordination	$1.6\text{--}6.2 \times 10^{-3}$ S/cm	3
5	PNIPAM/Lapointe/CNT	Hydrogen bonding	$1.3\text{--}1.9 \times 10^{-3}$ S/cm	4
6	Chitosan/PEG/PANI	Schiff base reaction	$2.25\text{--}3.5 \times 10^{-3}$ S/cm	5

^a FSWCNT: functionalized single wall carbon nanotubes; CMC: carboxymethyl cellulose; PDMA: poly(*N,N*-dimethyl acrylamide); PEG: Polyethylene glycol; PAMAA: poly(acrylamide-co-acrylic acid); PNIPAM: poly(*N*-isopropylacrylamide); PANI: polyanilin.

Reference

- 1 M. Liao, P. Wan, J. Wen, M. Gong, X. Wu, Y. Wang, R. Shi and L. Zhang, *Adv. Funct. Mater.*, 2017, **27**, 1703852.
- 2 H. An, Y. Bo, D. Chen, Y. Wang, H. Wang, Y. He and J. Qin, *RSC Adv.*, 2020, **10**, 11300-11310.
- 3 S. Liu, O. Oderinde, I. Hussain, F. Yao and G. Fu, *Polymer*, 2018, **144**, 111-120.
- 4 Z. Deng, T. Hu, Q. Lei, J. He, P. X. Ma and B. Guo, *ACS Appl. Mater. Interfaces*, 2019, **11**, 6796-6808.
- 5 X. Zhao, H. Wu, B. Guo, R. Dong, Y. Qiu and P. X. Ma, *Biomaterials*, 2017, **122**, 34-47.